# Chapter 2 Experiment

## 2.1 UHV chamber

All the experiments presented in this work were conducted in the UHV chamber designed by H. Bludau during his Ph.D. work [27]. The simplified top and side view of this chamber are shown in Fig. 2.1.

The chamber is pumped out by a turbo molecular pump (Varian, pumping speed = 100 l/s) that was connected to a rotary pump. In addition to the turbo molecular pump, a Ti sublimation pump was installed. The base pressure of this chamber was $3\times10^{-11}$ mbar. During measurements, the background pressure in the chamber was kept below $5\times10^{-10}$ mbar. The following instruments are housed in the UHV chamber.

– For sample cleaning, an Ar-ion gun (Varian) was installed in the chamber.

– An ion gauge with W filaments (V.G.) measures the pressure in the chamber. This ion gauge could operate only below a pressure of $5\times10^{-4}$ mbar.

– The quadrupole mass spectrometer (Balzers) was used with off-axis secondary electron multiplier (SEM) to analyze the composition of the background gas in the chamber and also to perform thermal desorption experiments.

– A Kelvin probe measures the work function change.

– A cylindrical Mirror Analyzer (CMA) with an electron gun (Perkin Elmers) in the middle of the analyzer was used for Auger electron spectroscopy (AES) measurements.

– A four-grid LEED optics with a $LaB_6$ filament (Prof. K. Müller, Erlangen, with Spectraleed-optics of Omicron) was used to analyze surface structures. A video camera was installed behind the screen of the back-view LEED.

– The gas shower that was developed by E. Piltz during the Ph.D. work of S. Schwegmann [26] was used to dose extraordinarily high amounts of gas (Fig. 2.2). In this system, gas molecules pass through a commercial multi-channel

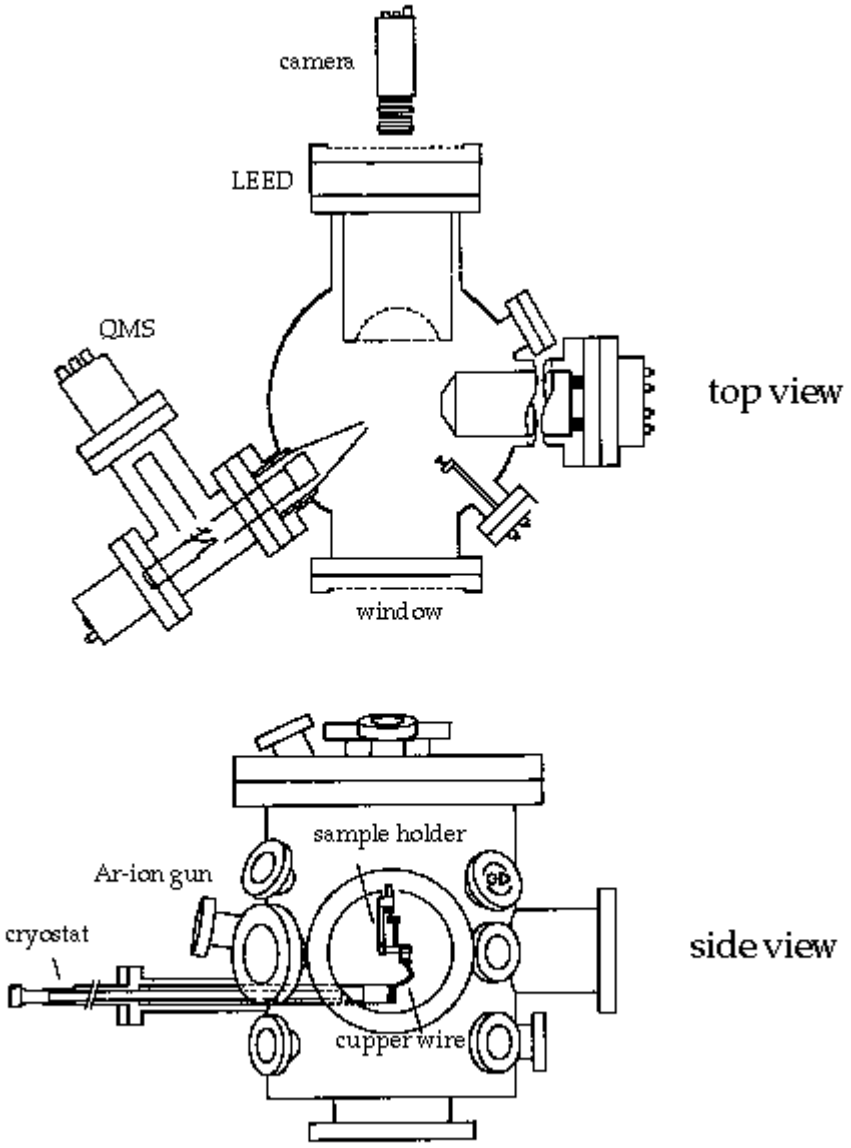


Fig. 2.1. Sketch of the UHV apparatus used in this work [27].

plate (with channels 3 mm long and 10 .m wide, total transparency of 50 %) so that the gas molecules are directed. The local pressure in front of the shower becomes much higher than the background pressure in the chamber. The local pressure in front of the multi-channel plate turned out to be about 100 times higher than the background pressure of the chamber [26].

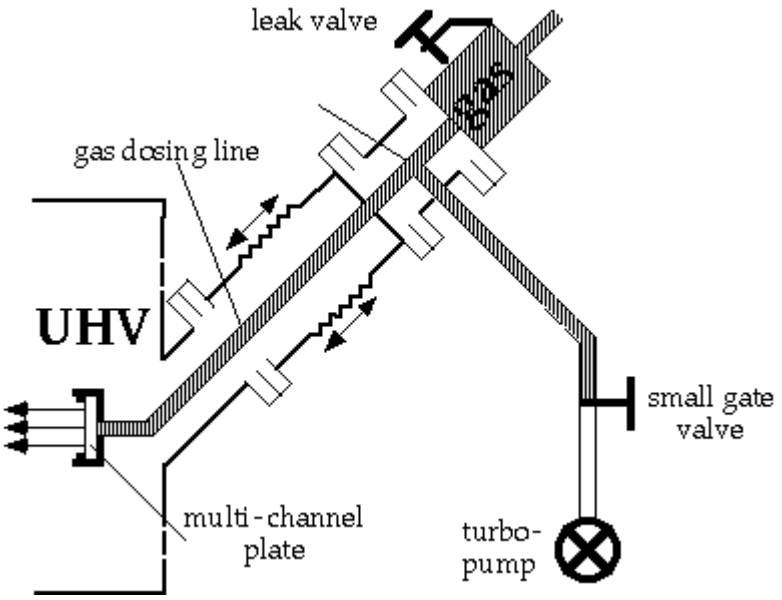


Fig. 2.2. Simplified sketch of the gas shower system [26].

– The Ru single crystals used in this work were disk-type with a thickness of about 2 mm. The highest sample temperature was 1550 K by direct resistive heating. With liquid He, the sample temperature could be lowered to 45 K and with liquid $N_2$ to 100 K. The sample temperature was measured with a NiCr-Ni-type thermocouple, which was spot-welded on the backside of the sample.

## 2.2 Experimental details

### 2.2.1 Thermal desorption spectroscopy (TDS)

The experimental procedure of TDS is the following: After a particular gas is exposed to a sample surface, the sample is heated with a constant heating rate, and the species that desorb from the surface are detected by a quadrupole mass spectrometer (QMS).

From thermal desorption experiments one can identify the desorption mechanism and determine the kinetic parameters, such as the desorption energy and the pre-exponential factor. Also, the qualitative analysis of thermal desorption spectra allows to determine the desorption order. In a first-order desorption, i.e., desorption of an adsorbate A to a gas molecule A(g), the peak temperatures of TD spectra are independent of the initial coverage of the adsorbate. In a recombinative desorption (A+A → $A_2$(g)), the peak temperature generally shifts to a lower temperature with increasing initial coverage. In the first-order desorption, one can determine the activation energy of desorption using the heating rate variation method [28].

### 2.2.2 Auger electron spectroscopy (AES)

The mechanism behind the Auger process is the following (Fig. 2.3) [29]:

a) A core level electron is emitted by electron radiation, and the atom is ionized.

b) An electron of an energetically higher level fills into the vacant core level.

c) The energy gain induced by process b) is transferred to a second electron to be emitted. This second electron is called the Auger electron. The kinetic energy of an Auger electron is given by

$$E = E_K - E_L - E_M \qquad (2.3.1)$$

where $E_I$ is the binding energy of the electron in level I.

A competing process to the Auger electron emission is the X-ray emission. Here, the energy gain resulted from process b) in Fig. 2.3 is emitted as an X-ray photon.

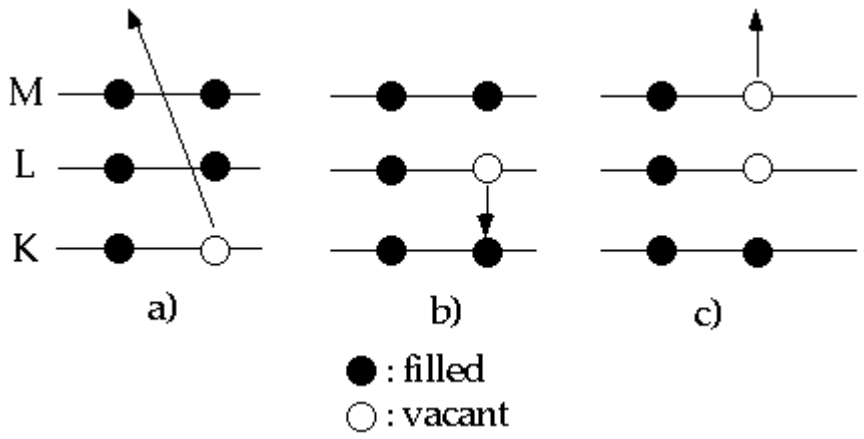


Fig. 2.3. Auger electron emission mechanism.

### 2.2.3 Low-energy electron diffraction (LEED)

In LEED optics, the electron gun delivers a monoenergetic beam with a typical kinetic energy of 40–400 eV to the single crystal surface. The electrons elastically backscatterred from the sample are accelerated (typically by 4 keV) on a fluorescence screen. The observed diffraction pattern reveals the translational symmetry and the point group of the surface in the reciprocal space [30, 31]. Since the mean free path of these electrons is only about 5 Å, LEED is surface sensitive [30, 31].

#### 2.2.3.1 Structure analysis by measuring and computing LEED I/E curves

The surface structure can be determined by quantitative LEED I/E analysis [30, 31]. One measures first the intensities of LEED beams as a function of the primary electron energy, so-called LEED I/E curves. The I/E curves of model structures are calculated by using the program code of Moritz [32, 33] and compared to the experimental I/E curves. The structural and nonstructural parameters for the models are optimized, until the agreement between experimental and simulated I/E curves does no longer improve. From the various models the model with the best agreement can be regarded as the correct one.

In this work, LEED I/E data were taken at the normal incidence of the primary electrons. For I/E measurements, a video-LEED system is utilized. Two different video systems were used in this work. The old video system (camera from Bischke) was utilized for the structure investigation of the Ru(0001)-(2×2)-3O phase (in chapter 3). All other measurements were performed with the new system (SensiCam from PCO).

In the old system, I/E curves were directly measured during the energy scan. The number of LEED beams, whose intensities as a function of energy can be measured at the same time, were limited to 8. In general, a data set of an adsorbate overlayer contains I/E curves from more than 50 LEED beams. Therefore, one has to iterate an energy scan more than 6 times to produce the complete data set for a structure. The old camera read out the intensity with 8 bit digitization (intensity value: 0–256). To measure I/E curves with this camera, the primary LEED beam current should be 100 nA–1000 nA.

Some molecules such as CO, $NH_3$ and hydrocarbons are damaged by the primary LEED beam. Consequently, the shape of the I/E curves changes while taking the I/E curves. To solve this problem, the time that a sample surface is exposed to the primary LEED beam (t) should be reduced. On the other hand, the camera should be more sensitive to LEED signals so that one should be able to measure I/E curves with a lower primary beam current (e). In summary, (t×e) should be reduced to achieve the I/E curves of the sensitive molecules as CO, $NH_3$ and hydrocarbons without damaging them. Due to the relatively high primary LEED beam current (100 nA–1000 nA) and long measuring time required, it is difficult to take the I/E curves of these sensitive molecules with the old system.

The new system with SensiCam solved this problem. In order to reduce data collection time, complete LEED images taken by SensiCam were transferred to the computer via a fiber optics cable. The pictures were saved on the hard disc of the computer. By taking LEED images at various energies (typically in 1 eV), one gets a ‘movie’ of the LEED patterns as a function of primary electron energy after an

energy scan. The time consuming step, analyzing the intensity information from more than 50 beams from the LEED screen, is separated from the actual data collection so that it is not necessary to expose the sample to the primary electrons for a long time. The actual data collection takes about 10 minutes with the new system, while about 1 hour is required with the old one.

The CCD chips of SensiCam read out the intensity with 12-bit digitization (intensity value: 0–4095). Therefore, longer exposure time can be used to take a LEED image (typical exposure time for a LEED image: 0.2 seconds), which can improve the quality of I/E curves. These CCD chips were cooled down to -15 °C so that the dark current (noise level) of this device is reduced. The sensor consists of 1280 x 1024 pixels. Several pixels can be grouped (binning) together, resulting in a higher sensitivity. Due to the increased sensitivity by longer exposure time, lower dark current and binning, the primary electron emission currents of 10 nA–100 nA were sufficient for collecting I/E curves with the new system.

To extract the I/E curves from the movie, a square window was set around a beam. The path of a beam as a function of the primary energy was defined before the ‘movie’ runs so that the window keeps track of the actual beam positions while changing the energy. Note, the LEED spots are moving radially towards the (0,0) beam when increasing the energy. The intensity of a beam was determined by the integral of the intensity inside the window, from which the background intensity (the intensity at the frame of the window) was subtracted. The intensity curve acquired in this way was normalized to the emission current of primary electrons. The I/E curves were then smoothed, and all the symmetrically equivalent beams were averaged. The I/E curves of symmetrically equivalent beams can actually be different due to the systematic errors such as an imperfect electron gun alignment or the presence of the external magnetic fields. These errors are reduced by averaging the I/E curves of the symmetrically equivalent beams.

In the computation of the LEED I/E curves, the multiple scattering is to be considered [30, 31]. Multiple scattering contributions are important in LEED due to

the strong scattering of electrons at the electrostatic potential imposed by the partially shielded positive charge ion cores. Therefore, the shape of I/E curves depends not only on the atomic scattering factor of adsorbates and substrate atoms but also on their local adsorption geometries [34].

The R-factor is used to quantify the agreement between two I/E curves. R is the abbreviation for 'reliability'. Various R-factors are used for determining the degree of the agreement between calculated and experimental LEED I/E curves. In the present work, the R-Pendry ($R_P$) factor [35] was used. Since $R_P$ is sensitive to small noise signals, experimental LEED I/E curves should be smoothed.

$R_P = 0$ is defined as a perfect agreement between two I/E curves. $R_P = 1$ indicates no correlation, and $R_P = 2$ anti-correlation between two I/E curves. In the case of clean single crystal surfaces, $R_P < 0.2$ indicates a nice agreement between theory and experiment. For an adsorbate system, $R_P$ about 0.25 can be accepted as a good agreement. For more complicated systems, for example in this work, oxide structures on Ru single crystals, $R_P$ below 0.4 can be regarded as an acceptable level of agreement between theory and experiment. $R_P$ higher than 0.5 indicates a bad agreement in any case.

For the automatic optimization of structural and non-structural parameters, the Marquardt algorithm [36, 37] has been implemented in the program of Moritz [32, 33].

In the program of Moritz, the x, y and z positions of the atoms, the Debye temperature and the occupation factor can be systematically or automatically varied. The symmetrization [38] was used in this program to save computing time and memory. Generally, the Debye temperatures of atoms located deeper than in the second layer were fixed at the bulk values found in the literature. The Debye temperatures of first and second layer atoms were refined.